Energy balance modelling of container farms with economizer cooling and heat recovery in remote microgrids

Francesco Ceccanti[a], Aldo Bischi, Andrea Baccioli

[a] Department of Energy, Systems, Territory and Construction Engineering, Università di Pisa, Pisa, Italy, destec@pec.unipi.it

Abstract:

Remote cold-climate communities often face limited access to fresh vegetables because local cultivation is constrained by harsh conditions, and supply chains are long and vulnerable. This work evaluates the techno-economic and environmental feasibility of a small container-based vertical farm for lettuce, benchmarked against imported produce purchased in a southern hub and delivered by refrigerated air freight. An agri-energy model is used to generate hourly electricity and heat-demand profiles for three configurations: baseline, air–water free cooling, and air–air free cooling. These load profiles are coupled with a mixed-integer linear programming formulation to optimize off-grid operation with a 12-kW diesel generator, a Li-ion battery, and an optional hot-water thermal energy storage. Free cooling can replace most compressor-driven cooling under Arctic-like conditions. The air-air strategy covers 96% of the annual cooling load and reduces specific electric energy consumption to 6.43 kWh_{el} kg^{-1}, 13% lower than the baseline, while annual electricity demand decreases from 58.9 to 51.3 MWh_{el}. The optimization identifies a 27-kWh battery to absorb surplus generation and avoid inefficient generator operation. Adding thermal storage shifts recovered heat to the dark period, reduced generator operating hours by about 12%, and yielded the lowest annual fuel use of 193.1 MWh. The integrated configuration combining air–air free cooling with electrical and thermal storage achieves the minimum annual energy cost and a simple payback of 1.5 years, with a 25% lower cost than imported lettuce. However, under diesel supply, the best case still emits 6.3 kg CO2e kg^{-1} versus 3.1 kg CO2e kg^{-1} for imports, and emissions parity requires low-carbon electricity to cover at least 51% of the farm energy demand. Therefore, the proposed solution becomes increasingly promising as remote microgrids progress along decarbonization pathways.

Keywords:

Vertical Farming; Energy System; Free Cooling; Remote Communities; Sustainability.

1. Introduction

Access to fresh vegetables in remote high latitude regions and other climatically harsh environments often depends on long and costly supply chains, with deliveries frequently constrained by limited transport options and seasonal disruption [1]. In communities without reliable year-round surface access, most perishable foods must be imported, and alternative routes or suppliers are often limited by geography, market size, and retail concentration. This dependence creates a structural constraint on affordability and the quality of fresh produce. The cost of nutritious diets in remote retail environments is shaped by high shipping and storage costs, and by the greater vulnerability of fresh items to deterioration during transport [2]. Socio-economic barriers are compounded by biophysical limits on local production. Short growing seasons, extreme temperatures, low winter solar radiation at high latitudes, permafrost or poor soils, and sparse infrastructure often make open field cultivation unreliable or infeasible. Overall, limited access to vegetables in remote communities is best understood as a food system problem in which logistics, energy, climate, and resilience jointly determine outcomes [3].

Vertical farming, defined here as indoor controlled environment agriculture using artificial lighting (PFAL) and hydroponics, is particularly suitable for short-cycle, high-density crops such as lettuce. It enables year-round production independent of outdoor climate, seasonality, and solar radiation, and it can reduce reliance on external supply chains for perishable produce. Canadian policy and sector analyses, including the Canadian Agri Food Policy Institute (2024) [4], describe vertical farming as a potential tool to strengthen fruit and vegetable availability in northern and remote communities, while emphasizing energy demand as a key constraint [4]. For deployment in remote settings, modular and container-based systems offer practical advantages because they can be shipped, installed quickly, and operated close to consumption points such

as schools, community centers, or small retailers [5]. The presence of commercial initiatives explicitly targeting northern markets with modular hydroponic units suggests that the approach is already being tested in practice and is moving toward early technology transfer [6].

Energy consumption is currently the primary bottleneck for vertical farming because it drives both operating expenditure and the climate footprint of the output. In many settings, electricity costs dominate the unit cost of leafy greens, and the associated emissions can offset, or even outweigh, the benefits expected from year-round local production and reduced transport. This is particularly relevant where the electricity mix is carbon-intensive or where power prices are high or volatile [7], conditions that are common in remote and northern grids.

Using lettuce as a reference crop, recent studies commonly report specific electricity use on the order of 10 to 18 kWh per kilogram, corresponding to roughly 850 to 1150 kWh per square meter per year [8]. In most energy balances, artificial lighting is the main load and typically accounts for about 64 to 85 percent of total demand. The remaining share is largely associated with environmental control, especially maintaining temperature and humidity within narrow ranges, plus auxiliary systems such as air circulation, pumping, fertigation, controls, and post-harvest handling. Humidity control is often nontrivial because plant transpiration creates a continuous latent load, so dehumidification and the management of condensation become central to stable operation. At the same time, heat generated by lighting must be removed, which links lighting decisions directly to cooling demand and, in some climates, to heating and heat recovery opportunities [9].

Techno-economics and modelling studies further show that energy use and cost per kilogram are highly sensitive to context. Outdoor conditions affect the HVAC burden, system design, and set points influence both crop yield and energy intensity, and local electricity tariffs and demand charges can change the cost structure substantially [10]. Consequently, the economic and environmental performance of vertical farming is not adequately captured by a single electricity use benchmark. Instead, it emerges from the coupled effects of crop strategy, system-level efficiencies, and control architectures, together with the local electricity context, including tariff structure, supply reliability, and grid carbon intensity. Consistent with this framing, recent reviews identify energy as the dominant constraint on scalability and emphasize the need for concurrent improvements in lighting and HVAC efficiency, integrated heat and moisture management, plant-responsive control of environmental set points and light regimes, and access to low-carbon electricity [7].

This study quantifies the energy feasibility of local lettuce production using container-based vertical farms in remote Canadian communities characterized by severe climates and electricity systems that are often isolated, costly, and capacity-constrained [11]. The core research question is whether, and under which technical and energy supply conditions, a container farm can operate reliably in these contexts, given that energy demand is widely recognized as the main technical and economic constraint for vertical farming and that performance depends critically on both the load profile and the characteristics of the available power system.

First, the annual electricity and thermal demand of a representative container farm is estimated through a detailed transient energy model [9]. The model is parameterized with lettuce growth and evapotranspiration requirements and runs over an entire year using site-specific climate data [12]. It explicitly accounts for the main end uses, including LED lighting, HVAC system (heating, ventilation, air conditioning), dehumidification, pumping, and auxiliary equipment, and converts crop targets and growth set points, including temperature, photosynthetic photon flux density (PPFD), and CO2 concentration, into time-varying internal heat and moisture loads and the corresponding energy needs. Cooling can remain relevant even in cold climates because lighting and equipment generate internal heat, and plants, through evapotranspiration, add a continuous moisture load that must be removed. To mitigate this demand, two outdoor air-based free cooling options are evaluated. The first uses an indirect configuration with an intermediate hydronic loop and an air-to-water heat exchanger, consistent with a water-side economizer. The second uses direct air-to-air heat exchange, consistent with an air-side economizer [13]. Both options are compared in terms of cooling energy reduction, controllability, and performance under cold and highly variable outdoor conditions.

Second, based on the resulting load profiles, an on-site generation system is modelled using a diesel-fueled generator designed to achieve full electrical self-sufficiency. The generator unit is coupled with an electrical battery to avoid operation below minimum stable load and to improve operational flexibility under variable demand. In selected scenarios, a thermal storage tank is included to increase the utilization of recovered heat, particularly for dark period space heating, and to reduce curtailment of useful thermal output. The joint dispatch of the generator unit and storage assets is optimized over a full year using mixed integer linear programming (MILP), enabling consistent estimation of primary energy use and production costs under different technology and fuel supply assumptions [14]. Finally, energy and cost metrics for local production are benchmarked against an import-based supply scenario, with explicit consideration of the expected differences in product freshness and quality that motivate local cultivation in remote settings.

2. Methods

This section describes the Agri-energy model used to predict energy consumption and crop productivity for a container farm located in Iqaluit, a town of about 7,740 inhabitants in the Nunavut Territory, Canada. The case

study considers a standard 12.03 m × 2.35 m × 2.69 m container [15] equipped with two growing racks comprising six tiers in total [16]. Each tier provides 13.2 m² of cultivable area, corresponding to 47% of the container floor area. The resulting total crop area is 79.2 m², which corresponds to a land use efficiency of 280% relative to the container footprint.

The container envelope is modelled using a typical layered assembly designed to limit heat losses under cold outdoor conditions. From outside to inside, the stratigraphy includes a 1.6 mm metal sheet, a 100 mm polyurethane foam insulation layer, and a 2.3 mm food-grade fibre reinforced polymer (FRP) liner. The calculated thermal transmittance of the opaque envelope is 0.22 W m^{-2} K^{-1}, with an additional 0.08 W m^{-2} K^{-1} assigned to thermal bridges [17].

2.1. Agri-Energy Model

The studied container farm uses an LED lighting system that delivers a constant photosynthetic photon flux density of 250 µmol m^{-2} s^{-1} over a 16 h photoperiod, corresponding to a daily light integral of 14.4 mol m^{-2} d^{-1}. The lamps are modelled with a photosynthetic photon efficacy of 2.5 µmol J^{-1}, resulting in an installed lighting load of approximately 8 kW.

Indoor climate is controlled by an HVAC system with a chiller for sensible and latent loads and an electric resistance heater for the dark period, when the LEDs are off. Temperature is maintained at 24 °C, with relative humidity set to 75% during the light period and 85% during the dark period. Resistive heating is assumed because heat pump performance is limited under Iqaluit's cold climate conditions. The growing chamber is CO_2-enriched to 1,200 ppm to enhance biomass accumulation [18]. Setpoints are taken from the sensitivity analysis reported in [7]. The Agri-energy model in [9] provides annual energy use and crop productivity for the benchmark, and performance is evaluated using the specific energy consumption (SEC) and the specific electric energy consumption (SEEC).

2.2. Free Cooling Strategies

Given that electricity demand is the main constraint in vertical farming, two free cooling strategies are investigated to reduce the cooling-related electrical load by leveraging low outdoor temperatures. Reducing insulation is not a viable alternative; indeed, while a non-insulated container can lower the sensible cooling requirement, it markedly increases the heating demand, which is met inefficiently with electric resistance, and it maintains or even increases the latent load associated with crop transpiration. In the insulated case, the chiller can address sensible and latent loads concurrently, whereas in the non-insulated case, humidity control remains necessary even when cooling demand is small, thereby offsetting most of the expected savings.

In the first configuration, a dry cooler (air-to-water heat exchanger) uses outdoor air to cool the chilled water loop from 12 °C to 7 °C. The unit is sized at an outdoor temperature of −3 °C, assuming a 10 °C air side temperature rise and a design heat duty of 8 kW. Off-design performance is modelled with an ε-NTU approach [19]. For each outdoor condition and required load, the outdoor air flow rate is iteratively determined. An initial air temperature rise is assumed to compute the air flow rate (Eq. 1), which is then used to update UA under off design conditions using the Dittus-Boelter correlation (Eq. 2). NTU and the heat capacity ratio C* are calculated and used to obtain the counterflow effectiveness ε (Eq. 3), from which the actual heat transfer rate and outlet air temperature are derived. The assumed air temperature rise is updated until convergence. Free cooling is enabled only when the outdoor temperature is at or below 2 °C. Above this threshold, cooling is provided by the compression chiller.

$$\dot{m}_{air,off} = \frac{Q_{off}}{1006 \cdot (T_{air,out} - T_{ext})} \quad (1)$$

$$UA_{off} = UA_{nom} \cdot \left(\frac{\dot{m}_{air,off}}{\dot{m}_{air,nom}}\right)^{0.6} \quad (2)$$

$$\varepsilon_{off} = \frac{1 - e^{-N \cdot (1 - C^*)}}{1 - C^* \cdot e^{-NTU \cdot (1 - C^*)}} \quad (3)$$

In the second configuration, free cooling is provided by an air-to-air heat exchanger that transfers heat from the warm, humid indoor air to the colder outdoor air stream. In addition to sensible cooling, the exchanger can also remove moisture by condensation on the indoor side whenever the indoor air is cooled below its dew point. The unit is sized at an outdoor temperature of 4 °C, assuming a 10 °C outdoor air temperature rise and a design heat duty of 8 kW. At design conditions, the indoor air is cooled from 24 °C to 12 °C. The outlet relative humidity approaches saturation at 12 °C, but the humidity ratio decreases because part of the water vapour condenses during cooling. To capture this behaviour, the heat exchanger is modelled with two consecutive sections. In the dry section, the indoor air is sensibly cooled from 24 °C down to its dew point temperature, which is computed from the inlet temperature and relative humidity. In the wet section, the indoor air is cooled from the dew point to 12 °C with simultaneous latent heat removal due to condensation. Moist air enthalpy is evaluated as a function of temperature and humidity ratio ω, so that the total heat transfer includes both sensible and latent contributions. Design effectiveness is defined as the ratio between the design heat duty and the maximum possible heat transfer rate. The corresponding NTU is obtained from the counterflow effectiveness relation (Eq. 4) and used to derive the design UA. Off-design operation is evaluated with the

same ε-NTU iterative procedure adopted for the first configuration, updating air flow rate, UA (Eq. 5), NTU, C*, and ε until convergence.

$$NTU = \frac{1}{1-C^*} \cdot ln \frac{1-\varepsilon}{1-\varepsilon \cdot C^*} \quad (4)$$

$$UA_{off} = UA_{nom} \cdot \left(\frac{\dot{m}_{air,in,off}}{\dot{m}_{air,in,nom}}\right)^{0.6} \cdot \left(\frac{\dot{m}_{air,ext,off}}{\dot{m}_{air,ext,nom}}\right)^{0.6} \quad (5)$$

Free cooling is enabled only when the outdoor temperature is at or below 8 °C to ensure net savings and limit fan power. For higher outdoor temperatures, the compression chiller supplies the cooling demand.

Fan electricity demand is estimated assuming a nominal heat exchanger pressure drop of 241 Pa. Under off-design operation, the pressure drop is adjusted using the quadratic relationship in Eq. 6. Part load fan efficiency is taken from [20] and applied to compute fan power for both configurations.

$$\Delta p_{off} = \Delta p_{nom} \cdot \frac{\dot{m}_{air,in,off}}{\dot{m}_{air,in,nom}} \quad (6)$$

2.3. MILP Formulation

The Agri-energy model, including the free cooling options described above, provides the hourly electric and thermal load profiles of the container farm over one year. Since Iqaluit is not connected to the national grid, electricity is supplied on site by a diesel-fueled generator set [11]. In both scenarios, a 12-kW unit is assumed and scheduled to meet the farm electrical demand [21].

A Li-ion battery is included primarily to manage the minimum technical load of the generator. The diesel unit cannot operate below 25% of rated power, while the farm demand might falls below this threshold. The battery therefore supplies the load during low demand hours and absorbs surplus generation when the generator is kept on, maintaining operation within admissible limits and reducing inefficient part load operation. Battery sizing and dispatch are obtained by minimizing the total annual energy cost (Eq. 8) through a mixed integer linear programming (MILP) problem solved in Gurobi. The MILP is formulated on an hourly horizon (8,760-time steps) with one binary on/off variable for the generator per time step (8,760 binary variables). In the first scenario, the formulation includes 43,803 continuous variables and enforces, at each time step, generator operating limits (rated power and minimum technical load), the electrical power balance, and battery state of charge dynamics. Battery state of charge is bounded between 20% and 90%, charge and discharge powers are limited by the battery nominal power, and round-trip efficiencies is set to 86% [22]. A cyclical constraint matches initial and final battery state of charge. Generator part load behaviour is represented through a convex piecewise linear approximation implemented with one additional constraint per time step (8,760 constraints) and no extra binary variables. Overall, the first scenario includes 70,083 constraints, plus 8,760 constraints associated with piecewise linearization.

$$f_{obj} = \sum_{t=1}^{8760} (FUEL \cdot c_{diesel} + \frac{CAPEX_{battery} \cdot CRF}{8760} + \frac{CAPEX_{TES} \cdot CRF}{8760} \quad (8)$$

A second scenario extends the MILP by modelling heat recovery from the diesel engine and a hot water thermal energy storage (TES). Additional constraints describe the hourly thermal balance, TES state of charge, bounds on TES capacity and charging and discharging powers, and cyclicity of the TES. Recoverable heat is defined as a function of generator operation and is allocated between direct use, TES charging, and curtailment. Thermal demand is met by recovered heat (directly or via TES discharge) and, when needed, by electric resistance heating, which increases the electrical load accordingly. TES charging and discharging efficiencies are set to 98% and 90%. This scenario comprises 105,125 continuous variables and 131,405 constraints, plus the same 8,760 piecewise linearization constraints. The two configurations are summarized in Figure 1. In both scenarios, investment costs for the battery and TES are modelled as functions of installed energy capacity and nominal power and annualized using a CRF based on a 6% interest rate and a 10-year lifetime.

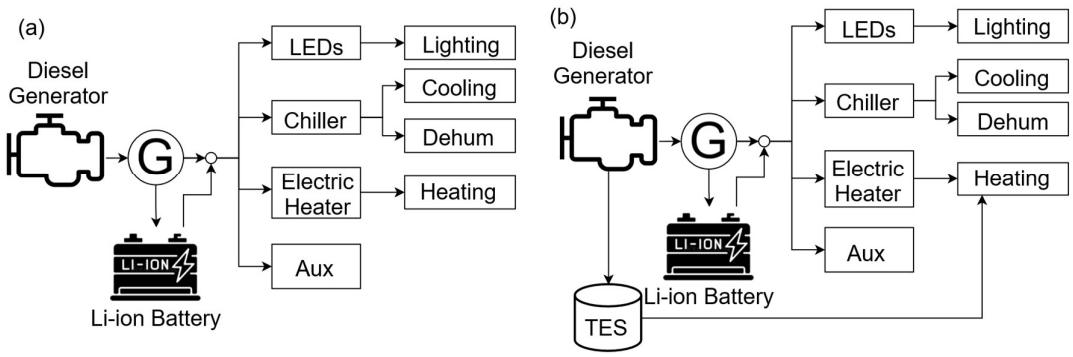

***Figure 1**: System architectures modelled in the MILP formulation. (a) Case 1: diesel-fuelled generator coupled with electrical battery storage. (b) Case 2: Case 1 extended with thermal energy storage.*

2.4. Economic and Environmental Assumptions

To evaluate cost competitiveness and environmental performance, a consistent set of assumptions is adopted for both the economic analysis and the greenhouse gas accounting. Table 1 reports the main economic inputs used in the optimization and post processing, including diesel fuel costs for the on-site generator and the capital expenditures for the electrical battery and the thermal energy storage. Cost results are reported per kilogram of marketable lettuce, and capital costs are annualized according to Eq. 8.

The benchmark is the current import-based supply option in Iqaluit. The total cost of locally produced lettuce, including energy and consumables such as packaging, seeds, and fertilizers, is compared against an import scenario in which lettuce is purchased in Ottawa and delivered to Iqaluit by refrigerated air freight. Labour costs are excluded because they are highly uncertain for a farm of this scale and context. To represent losses along the cold chain, a spoilage rate of 5% is assumed during handling and transport. Accordingly, costs and emissions associated with imported lettuce are allocated to the delivered, marketable fraction, corresponding to 95% of the shipped mass.

***Table 1**: Economic Assumptions.*

Parameter	Value	Unit	Reference
Fuel Cost	1.79	$ kWh^{-1}	[23]
Battery Cost per Power	375	$ kW^{-1}	[22]
Battery Cost per Energy	245	$ kWh^{-1}	[22]
TES Cost per Power	17.15	$ kW^{-1}	[24]
TES Cost per Energy	11.43	$ kWh^{-1}	[24]
Vertical Farm Operative Costs	1.14	$ kg^{-1}	[7]
Lettuce Cost in Ottawa	2.31	$ kg^{-1}	[25]
Air Transport Cost	4.05	$ kg^{-1}	[26]
Air Transport Cost (Tax Included)	4.36	$ kg^{-1}	[26]

For sustainability comparison, emissions for imported lettuce are estimated as the sum of a production footprint and transport-related emissions from Ottawa to Iqaluit. Conventional production is represented using an emission factor of 1.35 kg CO_2e per kg of lettuce [27]. Transport is modelled as refrigerated air freight over 2,270 km with an emission factor of 0.7 kg CO_2e per t-kilometre [28], followed by a 35 km last-mile leg by diesel truck with an emission factor of 0.101 kg CO2e per t-kilometre [28]. Consistent with the economic benchmark, emissions in the import scenario are allocated to the marketable fraction to account for the assumed 5% spoilage.

For local production, operational emissions are computed from the simulated electricity demand and a diesel generator emission factor of 0.26 kg CO_2e per kWh of fuel burned. The GHG assessment therefore focuses on operational and logistics-related emissions. Embodied emissions associated with infrastructure and consumables are excluded and discussed as a limitation.

3. Results and Discussion

This section presents the results of the analysis based on the assumptions and parameters defined in the Methods section. First, the impact of the two free cooling strategies on the container farm energy performance is quantified using the Agri-energy model. The resulting annual hourly electricity and thermal load profiles are then used as inputs to the MILP formulation, which determines the cost optimal scheduling of the diesel generator and the energy storage systems for each configuration. Finally, the best performing solutions are compared against a baseline import scenario, in which lettuce is supplied from a southern distribution center, in terms of both economic cost and greenhouse gas emissions.

3.1. Free Cooling Performance

The additional heat exchangers required by the two free cooling strategies were designed using the ε-NTU method, and the resulting design parameters and performance are reported in Table 2. For both configurations, the design external temperature was set 8 °C below the hot-side outlet temperature to avoid excessively large heat exchanger area.

Because of this higher design point, the air-air free cooler operates most of the time at outdoor temperatures lower than its design condition. As a result, the required outdoor air flow rate is typically lower than the design value, which reduces fan power consumption over a large share of operating hours.

Conversely, removing the intermediate hydronic loop reduces the overall heat transfer coefficient UA (-12.5%), The use of a compact plate-fin heat exchanger in the air-air configuration resulted in a slight reduction in capital cost, despite the larger heat transfer area. However, the higher pressure losses of the plate-fin heat exchanger led to a 20% lower EER in the air-air configuration compared to the air-water configuration. Over annual operation, however, the air-air configuration tends to exhibit a higher effective EER because it more frequently

operates below its design outdoor temperature, thereby benefiting from reduced air flow requirements and lower auxiliary fan demand.

***Table 2**: Design parameters, performance metrics, and estimated costs of the free cooling heat exchangers.*

Design Parameter	Air-Water	Air-Air	Unit
External Temperature	-3.0	4.0	°C
Outlet External Air Temperature	7.0	14.0	°C
Rated Heat Power	8,000	8,000	W
Heat Transfer Coefficient	1,220	1,049	$W\ K^{-1}$
Air Flow Rate	0.80	0.80	$kg\ s^{-1}$
Effectiveness	0.66	0.13 (dry) / 0.57 (wet)	[-]
Heat Transfer Area	11.4	17.2	m^2
Pressure Drop	50 (in) / 241 (out)	241 (in) / 241 (out)	Pa
Fan Power	286	353	W
EER	27.97	22.66	[-]
Cost	12,000	11,000	$

Different design outdoor temperatures lead to different free-cooling operating hours and, consequently, different chiller-load coverage (see Figure 2). The benchmark chiller load, defined as sensible cooling plus latent dehumidification, totals 36.2 MWh_{th}, which translates into 8.0 MWh_{el} (about 15% of the total farm electricity demand), implying an average chiller EER of 4.58 under the local climate conditions.

The air–water free cooling strategy covers 72% of the annual cooling and dehumidification demand, raising the average equivalent EER to 111.2 and reducing cooling-related electricity use to 2.8 MWh_{el}, 65% below the benchmark. Because lighting dominates total consumption, the overall impact is smaller, with SEEC decreasing from 7.37 to 6.68 $kWh_{el}\ kg^{-1}$, a 10% reduction.

The air–air free cooling strategy achieves higher coverage thanks to its higher design outdoor temperature, which keeps free cooling available even during warmer periods, including summer. It removes 34.5 MWh, of cooling and dehumidification load, covering 96% of the annual requirement. Electricity use for cooling and dehumidification drops to 0.7 MWh_{el}, which is 75% lower than the air–water case and 91% lower than the benchmark, yielding a SEEC of 6.42 $kWh_{el}\ kg^{-1}$. The average equivalent EER reaches 274 because the required outdoor airflow is low for most operating hours, and fan power remains limited despite reduced part-load efficiency.

Alternative free cooling concepts were excluded from the analysis. Direct ventilation of outdoor air into the growing chamber was not considered cost effective because it would increase CO_2 losses and risk cold drafts and local cold spots, requiring preheating or a large air–air heat recovery unit. Using cold seawater as a heat sink was also discarded because the required infrastructure would be disproportionate for a small-scale farm and local demand does not justify larger installations. Finally, the cost competitiveness of the proposed free cooling solutions depends on the on-site electricity cost, which is examined in the next section.

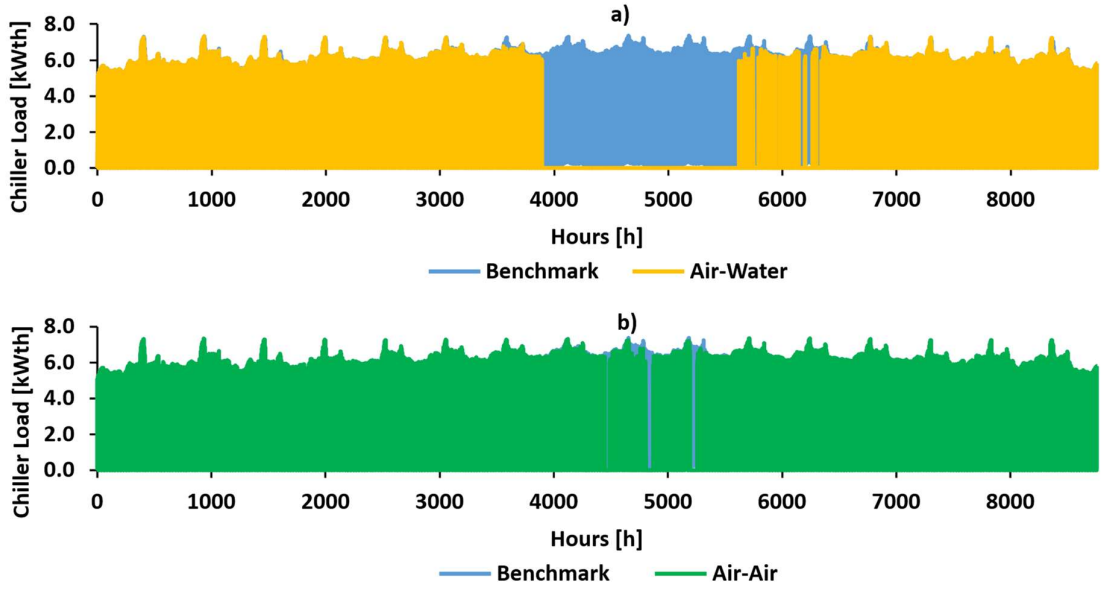

***Figure 2**: Cooling and dehumidification loads of the farm for the analyzed configurations. (a) Compressor-driven chiller versus air–water free cooling. (b) Compressor-driven chiller versus air–air free cooling.*

3.2. Case 1: Combination of Generator and Li-Ion Battery

The benchmark configuration yields an annual farm electricity demand of 58.9 MWh_{el}. Implementing free cooling reduces this demand to 53.4 MWhel with the air-water option and to 51.3 MWh_{el} the air-air option. For each case, the resulting hourly electrical load profile is provided to the MILP solver, which optimizes battery energy capacity and power rating to minimize the total annual energy cost while respecting the diesel generator operating constraints. Results are summarized in Table 3.

Across all three configurations, the optimized dispatch operates the 12-kW diesel generator close to its rated output, resulting in a similar average electrical efficiency of about 26%. When free cooling reduces the farm electricity demand, this strategy produces a larger surplus with respect to the instantaneous load. The surplus is routed to the Li-ion battery, which therefore becomes more heavily used and is sized larger as the farm demand decreases. Battery losses are treated as charge/discharge losses and are computed on an annual basis as the difference between total electricity generated and total electricity delivered to the load. Because SOC cyclicity is enforced over the year, this difference represents the net round-trip losses associated with storage utilization. Accordingly, the air-air case, having the lowest farm demand, exhibits the largest storage-related losses (about 4%) due to the higher energy throughput through the battery driven by the near-nominal generator operation.

Despite the higher battery investment required by free cooling configurations, both strategies reduce the overall annual energy cost. The air-water option achieves annual savings of 5.4% (approximately 2.3 k$ per year), while the air-air option achieves savings of 8.4% (about 3.5 k$ per year). Based on these operational savings, the simple payback time is 3.5 years for the air-air system. The air-water option, with lower savings and an investment cost of about 12 k$, results in a longer payback time (5.4 years).

***Table 3**: Optimized Case 1 system architecture and techno-economic performance.*

Optimized Parameters	Bench	Air-Water	Air-Air	Unit
Battery Capacity	23.0	25.0	27.0	kWh
Battery Power Rate	10.0	10.0	10.0	kW
Battery Nominal Duration	2.3	2.5	2.7	h
Electricity Produced	60.6	55.4	53.5	MWh_{el}
Fuel Required	232.6	212.6	205.5	MWh_{th}
Average Efficiency	26.0	26.0	26.0	[%]
System Losses	2.7	3.7	4.0	[%]
System Capex	9,400	21,875	21,365	[$]
Annual Energy Cost	41,640	39,360	38,150	$

The optimal dispatch strategy is illustrated in Figure 3, which shows the hourly electricity balance for a representative day in the air-air configuration. Because lighting is the dominant electrical end use, the load profile is largely dictated by the photoperiod and remains broadly similar throughout the year. Differences among configurations are therefore mainly driven by cooling-related electricity demand, which determines the amount of surplus energy that must be shifted through the battery.

The MILP avoids inefficient generator part-load operation by combining on/off scheduling with battery buffering. The generator is conservatively oversized relative to the average farm demand and, when committed, it is dispatched above the instantaneous load, with surplus electricity stored in the Li-ion battery. This effect is more pronounced under air-air free cooling because the reduced cooling demand lowers the net farm load and increases the surplus available for charging.

On the representative day, the battery is charged primarily during the lighting period and supplies the farm during low-load hours, allowing the generator to remain off for approximately 12 h. On an annual basis, the generator operates for 4,586 h (52%) with a part-load ratio of 97% over operating hours, indicating that it is typically dispatched near rated power when on. Overall, the battery supplies about 31% of the daily electrical demand and, when its state of charge is sufficiently high, it can cover the load even during portions of the LED light period. In the example shown, the LEDs are off between 10:00 and 18:00 and the battery fully supplies the electrical load.

The zero-heating demand immediately after lights switch off (at 10:00) reflects the thermal inertia of the enclosure and the hourly time step used in the MILP. With a 1 h resolution, short transients are averaged and the instantaneous heating requirement can be underestimated. A finer time step would improve the representation of short-term dynamics and the resulting dispatch, but it would substantially increase the computational burden of year-long optimization, making high-resolution scheduling more suitable for shorter analysis windows.

Finally, once free cooling is implemented, downsizing the generator could further improve cost competitiveness by reducing oversizing, although smaller units may exhibit slightly lower nominal efficiency.

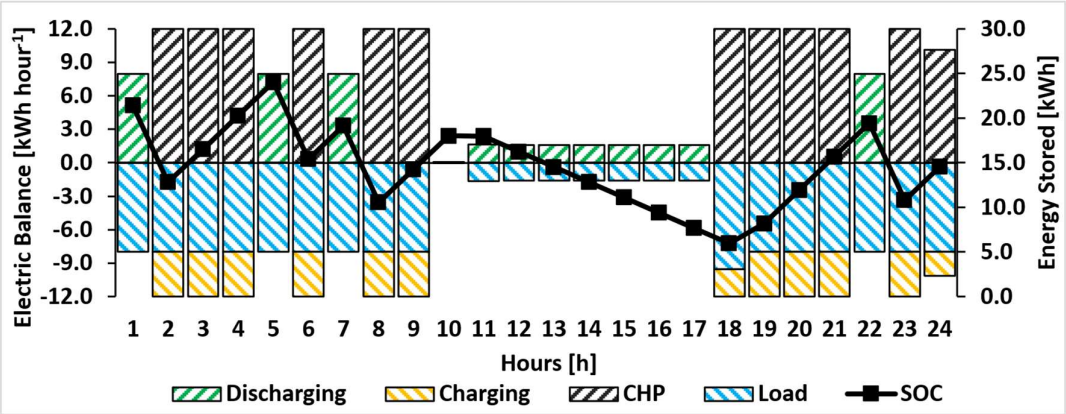

***Figure 3**: Typical daily dispatch of the diesel-fueled generator and Li-ion battery for the air–air free cooling configuration.*

3.3. Case 2: Combination of Generator, Li-Ion Battery and TES

In Case 2, the diesel generator is coupled with a hot-water thermal energy storage (TES) to reduce the farm electricity demand by shifting recovered heat to periods when heating is required. Despite the high insulation level, space heating still accounts for about 6% of the total electricity demand. Even partial recovery of the generator waste heat, buffered through an 18 kWh_{th} TES, yields measurable benefits. In the benchmark (no free cooling) configuration, the TES reduces the annual cost by about 4%, resulting in a simple payback of less than one year and indicating that thermal storage is a cost-effective option for small-scale off-grid vertical farms.

The TES also mitigates the need to cycle the Li-ion battery during the dark period to supply low-power heating loads. As a result, battery charge/discharge activity is reduced, and the associated electrical losses decrease to 2.3% of the total electricity produced. Consistently across all three configurations, adding TES lowers the optimal battery capacity and therefore reduces battery-related investment costs. The optimized TES energy capacity and discharge power correspond to an effective duration of about 8–9 h, matching the dark period when heating demand is concentrated.

From a system-level perspective, the MILP maintains generator operation close to the high-efficiency region, achieving an average electrical efficiency of about 26%. The combined adoption of TES and free cooling further reduces fuel use. In particular, the air-air free cooling configuration achieves the lowest fuel consumption, approximately 17% lower than the benchmark fully electric farm without free cooling.

Because TES has a substantially lower specific cost than Li-ion storage, its inclusion is economically advantageous in all scenarios. The best-performing option is the air-air free cooling case with TES, which reaches the minimum annual energy cost (34.8 k$) and annual savings of 6.8 k$. Considering an additional investment of 10.45 k$ compared to Bench (case 1), the resulting simple payback is approximately 1.54 years.

***Table 4**: Optimized Case 2 system architecture and techno-economic performance.*

Optimized Parameters	Bench	Air-Water	Air-Air	Unit
Battery Capacity	17.0	21.0	20.0	kWh
Battery Power Rate	10.0	10.0	10.0	kW
Battery Nominal Duration	1.7	2.1	2.0	h
TES Capacity	18.0	16.0	17.0	kWh
TES Power Rate	2.0	2.0	2.0	kW
Electricity Produced	56.7	51.9	50.0	MWh_{el}
Fuel Required	219.2	200.0	193.1	MWh_{th}
Average Efficiency	25.8	26.0	25.9	[%]
System Efficiency	2.3	3.5	4.0	[%]
System Capex	8,140	21,100	19,850	[$]
Annual Energy Cost	39,920	36,580	34,800	$

The optimal dispatch for the Case 2 architecture is illustrated in Figure 4, which reports the hourly electricity and thermal balances for a representative day in the best-performing configuration (air–air free cooling). In this case, the electrical heating demand that would otherwise occur during the dark period (10:00-18:00) is largely replaced by a thermal demand that is met by discharging the hot-water thermal energy storage (TES), previously charged during the light period. This behavior reflects the limited simultaneity between electrical and thermal loads. The electrical demand is dominated by LED lighting and the associated cooling

requirements to remove waste heat, whereas space-heating demand becomes relevant mainly when the LEDs are off, i.e., when electrical consumption is lowest.

When neither TES charging nor battery charging is strictly required, the scheduler reduces the generator set-point to about 75% of rated power. At this operating level, the generator efficiency penalty is limited (approximately 6% relative to full-load efficiency), while avoiding unnecessary battery cycling is beneficial because electrical storage round-trip losses are on the order of 14%. Consistently, the battery is used slightly less than in Case 1, supplying about 28% of the daily electrical demand. Nevertheless, storage remains effective in reducing generator operating hours, which decreases to 4,401 h per year (50%). When operating, the generator is still dispatched close to rated conditions, with an average part-load ratio of 95%, slightly lower than in Case 1.

From a thermal perspective, the presence of TES avoids the low-efficiency conversion of electricity into heat via resistive heating across the year. However, the imbalance between heat demand and power demand limits the utilization of recovered heat. As a result, the average overall first-law efficiency of cogenerative architecture remains close to electrical efficiency, reaching 26.6%, which supports economic feasibility but indicates that the thermal recovery provides a modest improvement under the low heating-load conditions of the insulated container.

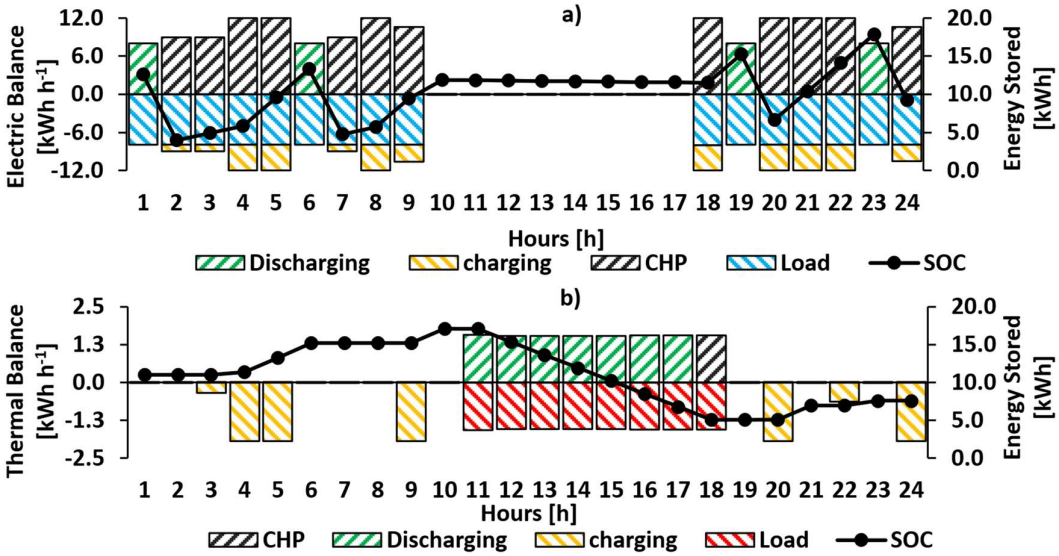

***Figure 4**: Typical daily dispatch of the diesel-fuelled generator, Li-ion battery, and hot-water thermal energy storage for the air-air free cooling configuration, showing the electrical balance (a) and thermal balance (b).*

3.4. Cost-Competitiveness and Sustainability

Based on the assumptions described in the Methods section, the cost-competitiveness and environmental performance of locally produced lettuce were benchmarked against imported lettuce using two indicators. The first is the production cost per kilogram of harvested lettuce (excluding labour), while the second is the specific greenhouse-gas footprint, expressed as kg CO2e per kg of lettuce.

From an economic standpoint (Fig. 5a), local vertical-farm production is more cost-competitive than imports, mainly because remote communities without year-round road access rely on long and expensive supply chains. The best-performing configuration (air-air free cooling combined with hot-water thermal energy storage) achieves a production cost of 5.50 \$ kg^{-1}, corresponding to savings of 25% relative to the import scenario and 13% relative to a fully electric vertical farm without free cooling. Although including labour could reduce this margin, the results indicate that container-based production can represent an economically viable option to improve access to fresh and healthy food in remote communities where food prices are structurally higher than in southern urban centres.

From an environmental standpoint, all scenarios show higher emissions than imports under the current diesel-based electricity supply. The combination of the high carbon intensity of diesel generation, the limited scale-related efficiency of small generators, and the constrained utilization of recovered heat results in specific emissions that remain substantially above the import baseline. Even the most energy-efficient configuration emits more than twice the imported option (6.30 vs 3.10 kg CO2e kg^{-1}). At present, Iqaluit, like many remote Canadian communities, is supplied by diesel-powered microgrids. However, several decarbonization pathways are actively being explored, including hybrid microgrids that combine renewables, electrical storage, and diesel

backup, as well as biomass-based solutions (e.g., coupled with small-scale ORC), hydrogen-based seasonal storage, and small modular reactors.

As remote grids progressively decarbonize, local production is expected to become increasingly attractive both economically and environmentally. Under the emission factors assumed here, the break-even condition for local production to match the import footprint is reached when low-carbon electricity supplies at least 51% of the farm's total energy demand.

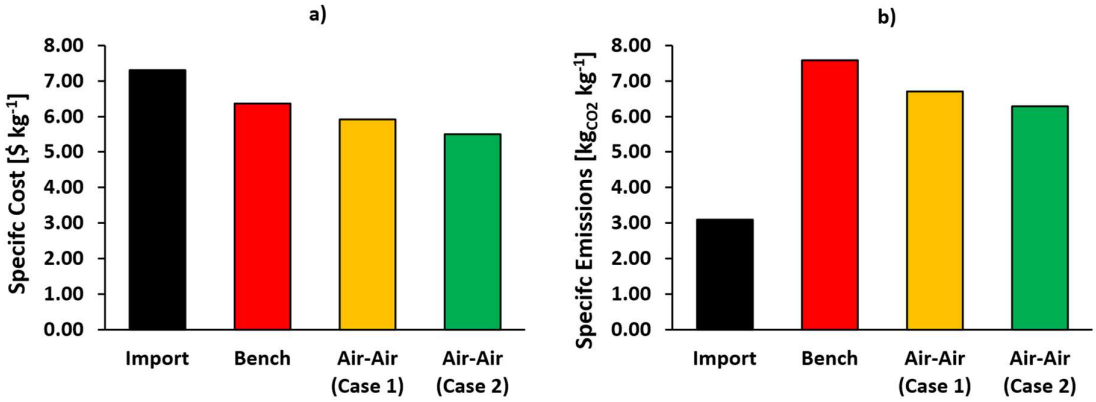

***Figure 5**: Comparison of vertical farm scenarios and imported lettuce in terms of economic and environmental performance.*

4. Conclusions

This study assessed the suitability of a small-scale container farm to supply fresh leafy vegetables to remote communities where open-field cultivation is constrained by low solar availability and extreme outdoor temperatures. Local production was benchmarked against imported lettuce by accounting for purchase and transport costs and for emissions associated with refrigerated air freight. To address the main limitation of vertical farming, namely high energy intensity, two free-cooling concepts were modelled to exploit cold outdoor temperatures and reduce cooling electricity demand. The resulting hourly load profiles for three configurations (baseline, air-water free cooling, and air-air free cooling) were then used as inputs to a MILP framework to optimize the dispatch of an off-grid diesel generator and the sizing of electrical and thermal storage. Key findings are summarized in the following bullet points:

- Free cooling is highly effective in cold climates. The air-air free cooling option provides the highest cooling coverage, reaching 96% of the annual cooling load, and reduces the farm specific electric energy consumption to 6.43 kWh_{el} kg^{-1}, which is 13% lower than the baseline. On an annual basis, total electricity demand decreases from 58.9 to 51.3 MWh_{el} from the baseline to the air-air case.
- Electrical storage is essential for off-grid operation with a minimum-load generator. Coupling the diesel generator with a Li-ion battery enables operation near the high-efficiency region despite a highly variable load profile. In the optimized solution, a 27-kWh battery reduces generator operating hours, and lowers the annual energy cost.
- Thermal energy storage improves system performance and reduces battery dependence. Adding hot-water TES shifts recovered heat to the dark period, replacing resistive electric heating, and reducing battery cycling. The TES decreases generator operating hours by about 12% and yields the lowest annual fuel use 193.1 MWh. It also reduces the optimal battery capacity from 27 kWh to 20 kWh, further decreasing annual costs.
- The combined solution is financially attractive. The configuration integrating air-air free cooling with both electrical and thermal storage achieves the lowest annual energy cost and a short simple payback time of 1.5 years, making it the most cost-effective option among those investigated.
- Economic viability is not currently translated into lower emissions under diesel supply. While local production is cost-competitive in this case study, with a 25% lower cost than imported lettuce, the diesel-based energy supply leads to higher emissions than the import baseline with 6.3 versus 3.1 kgCO2e kg^{-1}. Under the assumed emission factors, local production matches the import footprint only when low-carbon electricity supplies at least 51% of the farm energy demand, indicating that decarbonization of remote microgrids is required for vertical farming to deliver both cost and emissions benefits.

Nomenclature

c cost, $/MWh

C^* thermal capacity ratio, (-)

$\dot{m}$ mass flow rate, kg/s

p Pressure, Pa

P Electric Power, kW_{el}

Q Thermal Power, kW_{th}

T temperature, °C

UA Overall heat transfer coefficient, W/K

Greek symbols

η efficiency

ρ density, kg/m^3

ε effectiveness

Subscripts and superscripts

ext external

in inlet

nom nominal

obj objective

off off design

out outlet

References

[1] Health & wellbeing Queensland, “Remote Communities Healthy Food Supply Chain Study,” 2022. Accessed: Mar. 06, 2026. [Online]. Available: https://hw.qld.gov.au/wp-content/uploads/2023/12/Remote-Community-Supply-Chain-Study.pdf

[2] K. Tiff-Annie *et al.*, “Unintended consequences: food prices increase in an Arctic indigenous community amidst road infrastructure development and loss of federal freight subsidy,” *Front. Nutr.*, vol. 12, May 2025, doi: 10.3389/fnut.2025.1521800.

[3] A. Unc *et al.*, “Arctic food and energy security at the crossroads,” *Commun. Earth Environ.*, vol. 6, no. 1, p. 121, Feb. 2025, doi: 10.1038/s43247-025-02122-6.

[4] M. C. R. Pereira, K. Balaj, L. Atagher, and M. Adde, “A roadmap to support decision making on the implementation of vertical farming in Canada,” May 2024.

[5] C. Anderson, “Why this First Nation bought a shipping container during COVID-19.” Accessed: Mar. 06, 2026. [Online]. Available: https://www.tvo.org/article/why-this-first-nation-bought-a-shipping-container-during-covid-19

[6] Gouvernement du Canada, “Naurvik project in Nunavut.” Accessed: Mar. 06, 2026. [Online]. Available: https://www.asc-csa.gc.ca/eng/sciences/food-production/naurvik-project-in-nunavut.asp

[7] F. Ceccanti, A. Bischi, U. Desideri, and A. Baccioli, “Beyond yield: integrating energy, water, cost, and carbon to benchmark indoor vertical farming viability,” *Energy Convers. Manag.*, vol. 348, p. 120646, Jan. 2026, doi: 10.1016/j.enconman.2025.120646.

[8] L. Miserocchi and A. Franco, “Benchmarking energy efficiency in vertical farming: Status and prospects,” *Thermal Science and Engineering Progress*, vol. 58, p. 103165, Feb. 2025, doi: 10.1016/j.tsep.2024.103165.

[9] F. Ceccanti, G. Di Lorenzo, A. Bischi, L. Incrocci, A. Pardossi, and A. Baccioli, “A Transient Energy-Agriculture Model to Predict Energy Footprint of Vertical Farms,” *Energy Convers. Manag.*, Accessed: Feb. 17, 2025. [Online]. Available: Currently under review

[10] A. Arcasi, A. W. Mauro, G. Napoli, F. Tariello, and G. P. Vanoli, “Energy and cost analysis for a crop production in a vertical farm,” *Appl. Therm. Eng.*, vol. 239, p. 122129, Feb. 2024, doi: 10.1016/j.applthermaleng.2023.122129.

[11] Statistics Canada, “Market Snapshot: Clean Energy Projects in Remote Indigenous and Northern Communities,” Nov. 2023. Accessed: Mar. 10, 2026. [Online]. Available: https://www.cer-rec.gc.ca/en/data-analysis/energy-markets/market-snapshots/2023/market-snapshot-clean-energy-projects-remote-indigenous-northern-communities.html

[12] EU Science Hub, “Photovoltaic Geographical Information System.” Accessed: Apr. 17, 2025. [Online]. Available: https://re.jrc.ec.europa.eu/pvg_tools/en/

[13] Pacific Northwest National Laboratory, “Best Practices for Air-Side Economizers Operation and Maintenance.” Accessed: Mar. 10, 2026. [Online]. Available: https://www.pnnl.gov/projects/om-best-practices/air-side-economizers

[14] T. SHEKARI, A. GHOLAMI, and F. AMINIFAR, “Optimal energy management in multi-carrier microgrids: an MILP approach,” *Journal of Modern Power Systems and Clean Energy*, vol. 7, no. 4, pp. 876–886, Jul. 2019, doi: 10.1007/s40565-019-0509-6.

[15] Shipping Container Services, “Shipping Container Dimensions - Complete Size Guide”, Accessed: Mar. 11, 2026. [Online]. Available: https://shippingcontainerservices.com.au/shipping-container-dimensions/

[16] Food and Agriculture Organization of the United Nations, “‘Container Farming’ for High-tech Lettuce Cultivation.”

[17] M. Lawson and G. Vannier, “Thermal bridging in steel framed buildings.” Accessed: Mar. 11, 2026. [Online]. Available: https://www.newsteelconstruction.com/wp/wp-content/uploads/TechPaper/1410NSCtech.pdf

[18] D. Chen, J. Zhang, Z. Zhang, Y. Lu, H. Zhang, and J. Hu, “A high efficiency CO2 concentration interval optimization method for lettuce growth,” *Science of The Total Environment*, vol. 879, p. 162731, Jun. 2023, doi: 10.1016/j.scitotenv.2023.162731.

[19] L. Cabezas-Gómez, H. A. Navarro, and J. M. Saíz-Jabardo, “Theoretical Development,” 2015, pp. 9–21. doi: 10.1007/978-3-319-09671-1_2.

[20] AEROVENT, “Fan Performance Characteristics of Axial Fans.”

[21] Kubota, “Kubota Generators J112.” Accessed: Mar. 12, 2026. [Online]. Available: https://generator.kubota.com/products/50hz/j_112.html

[22] C. Augustine and N. Blair, “Energy Storage Futures Study: Storage Technology Modeling Input Data Report,” 2024.

[23] Government of Northwest Territories, “Fuel Prices effective ,” 2025, Accessed: Mar. 12, 2026. [Online]. Available: https://www.inf.gov.nt.ca/en/services/fuel-services/prices

[24] Energy Storage, “Technology: Sensible Heat Water Storage,” 2024. Accessed: Mar. 12, 2026. [Online]. Available: https://iea-es.org/wp-content/uploads/public/FactSheet_Thermal_Sensible_Water_2024-07-10.pdf

[25] A1 Cash+Carry, “Fresh - Lettuce - Romained.” Accessed: Mar. 12, 2026. [Online]. Available: https://www.a1cashandcarry.com/products/fresh-lettuce-romaine

[26] Canadian North, “Domestic Cargo Tariff Rates,” 2024, Accessed: Mar. 12, 2026. [Online]. Available: https://canadiannorth.com/wp-content/uploads/2024/10/Tariff_Corporate_Discount-for-15Oct24-Q4-New-Discount-Levels.pdf

[27] C. Chaudron, G. Martineau, and J.-A. Chayer, “Bilan environmental de la production de légumes de serre du Québec,” 2021. Accessed: Mar. 12, 2026. [Online]. Available: https://www.serres.quebec/wp-content/uploads/2025/02/groupe-ageco_bilan-environnement-production-legumes-serre-quebec_2021-09.pdf

[28] A. Lewis, S. Greene, and S. Punte, “Global Logistics Emissions Council Framework for logistics emissions accounting and reporting,” 2019.